Chemical Engineering Science 127 (2015) 269–275

Contents lists available at ScienceDirect

Chemical Engineering Science

journal homepage: www.elsevier.com/locate/ces

Partial oxidation of methane using silver/gadolinia-doped ceria composite membranes

E. Ruiz-Trejo [a,*], P. Boldrin [a], J.L. Medley-Hallam [a], J. Darr [b], A. Atkinson [c], N.P. Brandon [a]

[a] Department of Earth Science and Engineering, Imperial College London, London SW7 2AZ, UK
[b] Department of Chemistry, University College London, 20 Gordon Street, London WC1H 0AJ, UK
[c] Department of Materials, Imperial College London, London SW7 2AZ, UK

HIGHLIGHTS

- Novel Ag/CGO membranes fabricated with low metal content.
- Methane was partially oxidised using oxygen permeated through a Ag/CGO membrane.
- The membranes were stable in very low partial pressures of oxygen.
- No carbon deposition was observed in the membranes.

GRAPHICAL ABSTRACT

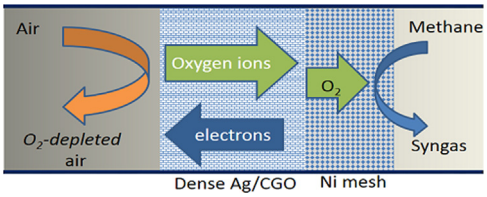

ARTICLE INFO

Article history:
Received 6 October 2014
Received in revised form
8 January 2015
Accepted 12 January 2015
Available online 2 February 2015

Keywords:
Methane partial oxidation
Cermet membrane
Silver
Gadolinia-doped ceria
Oxygen separation

ABSTRACT

Methane was partially oxidised to CO using oxygen permeated through a 1 mm thick silver/$Ce_{0.9}Gd_{0.1}O_{2-x}$ (Ag/CGO) composite membrane operating at 500–700 °C with air at 1 bar pressure. The membranes were fabricated by sintering ultrafine nanoparticles of gadolinia-doped ceria (< 5 nm) coated with silver using Tollens' reaction. This unique combination led to dense composites with low content of silver (7 vol%), no reaction between the components and predominant metallic conductivity. When feeding 4% methane at 700 °C to a 1-mm thick Ag/CGO using Ni as reforming catalyst, the conversion reached 21% and the CO selectivity 92% with an estimated oxygen flux of 0.18 mL min^{-1} cm^{-2} (NTP). The samples were stable in carbon-containing atmospheres and under a large pO_2 transmembrane pressure difference at temperatures below 700 °C for 48 h.

1. Introduction

Syngas, a mixture of carbon monoxide and hydrogen, is used for the production of synthetic fuels via the Fischer–Tropsch process or transformed into other chemicals, for example dimethyl ether (DME) (Sousa-Aguiar et al., 2011). Syngas is commonly produced on a large scale from methane by steam reforming, a method that requires large amounts of energy as the reaction is endothermic (Eq. (1)). The reaction also leads to a H_2/CO ratio of 3, higher than the ideal H_2/CO ratio of 2 necessary for further conversion to synthetic fuels (Sousa-Aguiar et al., 2011; Rostrup-Nielsen et al., 2002). Another method for the conversion of CH_4 is dry or CO_2 reforming, also an energy intensive process that yields a lower H_2/CO ratio of 1 (Eq. (2)) [2].

An ideal process to achieve the preferred H_2/CO ratio of 2 is the partial oxidation of methane. One way of achieving this is autothermal reforming, where a mixture of methane and oxygen is raised to a temperature of 1300 °C at which thermodynamic equilibrium favours the formation of syngas. The main disadvantages of this method are the high temperature and the need for high purity oxygen to hinder side reactions between nitrogen and the other components.

Catalytic partial oxidation on a mixed ionic–electronic membrane has been proposed to solve this problem (Yu et al., 2014; Balachandran et al., 1995). In practice, rather than direct partial oxidation, it is a two-step process. The first step is the complete

* Corresponding author. Tel.: +44 207 594 9695; fax: +44 207 594 7444.
E-mail address: enrique.ruiz-trejo@imperial.ac.uk (E. Ruiz-Trejo).

http://dx.doi.org/10.1016/j.ces.2015.01.047

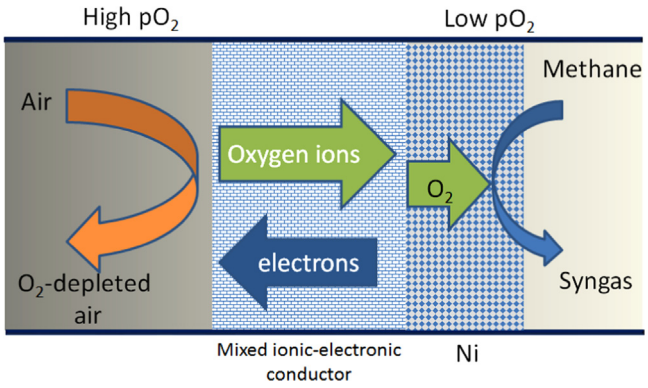

Fig. 1. Using a mixed oxygen ionic–electronic membrane, oxygen from air is incorporated into the ionic crystal lattice. Oxygen diffuses across the gas-impermeable membrane driven by a gradient in the chemical potential of oxygen. In the case of a composite membrane, oxygen migrates as oxygen ions through the ionic material and electrons are transported in the opposite direction mainly through the electronic conductor network. On the reducing side of the membrane the permeating oxygen then reacts with methane in the presence of a reforming catalyst to form syngas.

oxidation of methane to CO_2 (Eq. (3)) that provides the energy necessary for the second step, dry-steam reforming in the presence of nickel and excess methane. To be thermally efficient the energy released in the full oxidation step must be consumed in the reforming reactions. By combining Eqs. (1), (2) and (3), partial oxidation of methane to syngas produces the ideal H_2/CO ratio of 2 as shown in Eq. (4).

$$\text{Steam reforming } CH_4 + H_2O \rightarrow CO + 3H_2 \quad \Delta H_R^\circ = +206 \text{ KJ mol}^{-1} \quad (1)$$

$$\text{Dry reforming } CH_4 + 2CO_2 \rightarrow 2CO + 2H_2 \quad \Delta H_R^\circ = +247 \text{ KJ mol}^{-1} \quad (2)$$

$$\text{Complete oxidation } CH_4 + 2O_2 \rightarrow CO_2 + 2H_2O \quad \Delta H_R^\circ = -803 \text{ KJ mol}^{-1} \quad (3)$$

$$\text{Partial oxidation } CH_4 + \tfrac{1}{2}O_2 \rightarrow CO + 2H_2 \quad \Delta H_R^\circ = -36 \text{ KJ mol}^{-1} \quad (4)$$

Previous literature reports have shown that methane can also be partially oxidised using the permeated oxygen from air in a gas separation membrane operating above 800 °C in the presence of a reforming catalyst (Balachandran et al., 1995; Dyer et al., 2000; Shao et al., 2001), as illustrated schematically in Fig. 1.

Oxygen can be separated from air using a mixed ionic–electronic membrane that provides both oxygen transport and electronic conductivity (Yu et al., 2014; Dyer et al., 2000; Shao et al., 2001; Bouwmeester and Burggraaf, 1996; Dong et al., 2001; Teraoka et al., 1985; Ruiz-Trejo et al., 2014). A mixed ionic–electronic membrane can either be a composite, with separate electronically conductive and ionically conductive phases such as silver/$Ce_{0.8}Sm_{0.2}O_{2-x}$ (Ag/CSO) (Ruiz-Trejo et al., 2014), silver/copper oxide/gadolinia-doped ceria (Ag/CuO/CGO), CGO/$La_{1-x}Sr_xCo_{1-y}Fe_yO_{3-d}$ (LSCF) (Samson et al., 2014), or a single phase material in which both electrons and oxygen ions are mobile, such as LSCF (Teraoka et al., 1985) or $Ba_{0.5}Sr_{0.5}Co_{0.8}Fe_{0.2}O_{3-d}$ (BSCF) (Shao et al., 2000). Perovskite-based materials such as LSCF and BSCF have shown high permeation rates at high temperatures (800–1000 °C).

BSCF, one of the materials that has attracted more interest, is nonetheless strictly limited to operation at pO_2 above 10^{-5} bar, therefore limiting its use in hydrocarbon atmospheres (Vente et al., 2006); it is also known that oxygen permeation is greatly reduced in the presence of CO_2, due to carbonate formation, and even though the carbonation process might be reversible, use in carbon-containing atmospheres is further restricted by the complexity of operation (Arnold et al., 2007; Bucher et al., 2008). Although a variety of strategies have been implemented to solve these problems, the stability of BSCF is the main challenge for its long term operation under highly reducing and carbon containing atmospheres.

Herein, we present a metal–ceramic composite for *in-situ* oxygen production or partial oxidation of methane operating in the temperature range: 500–700 °C where economic heat sources can be used and with good tolerance to carbon containing atmospheres and good mechanical stability. The two main components are $Ce_{0.9}Gd_{0.1}O_{1.95}$ (CGO) as the ionic conductor and silver as the electronic conductor, labelled hereafter as Ag/CGO.

CGO has been shown to be catalytically active for both steam and dry reforming (Ramirez-Cabrera et al., 2002; Ramírez-Cabrera et al., 2004) and it exhibits high oxygen ion conductivity. Doped ceria-based materials are stable in carbon containing atmospheres and their high oxygen storage capacity is useful in ceria–zirconia solid solutions for exhaust gas cleaning (Ozawa et al., 1993).

Silver is an excellent catalyst for the reduction of oxygen and its additon to CGO increases the oxygen surface exchange coefficient by orders of magnitude (Ruiz-Trejo et al., 2014; Seeharaj and Atkinson, 2011). Silver is also considerably cheaper than Pt, Pd or other metals used in similar membranes (Sunarso et al., 2008). Furthermore, silver is also catalytically active for partial oxidation reactions (Nagy and Mestl, 1999).

In this work the composite membrane was fabricated by coating ultrafine CGO particles (5 nm) produced by continuous hydrothermal flow synthesis (CHFS), with silver followed by careful sintering. We demonstrate the selective permeation of oxygen through such a membrane, confirming our earlier report (Ruiz-Trejo et al., 2014) and then further demonstrate the effectiveness of such a membrane for the partial oxidation of methane using nickel as a reforming catalyst.

2. Experimental

The nanoparticles from which the membranes were fabricated, were produced by CHFS. A single aqueous solution of ammonium cerium nitrate (0.45 M) and gadolinium nitrate (0.05 M) (pumped at a flow rate of 200 mL min^{-1}) was mixed in line with an aqueous solution of KOH (0.5 M) at a flow rate of 200 mL min^{-1} before being mixed with a stream of water at 450 °C and 24.1 MPa flowing at 400 mL min^{-1} in a co-current mixer as described elsewhere (Tighe et al., 2013). The CGO nanoparticles were precipitated instantly, and the stream was then cooled and the pressure reduced to ambient by passing the products through a back pressure regulator. The particles were then separated by centrifuging the initial solids and cleaning the concentrated sludge by placing it in a dialysis bag in a large plastic vessel and replacing with clean water several times in the vessel. Once cleaned, the wet sludge was freeze dried overnight.

The dried particles were then silver coated using Tollens' reagent (Ruiz-Trejo et al., 2014; Tollens, 1882). In a typical experiment concentrated NH_4OH was gradually added to a solution of $AgNO_3$ (0.1 M), the addition was stopped when the black precipitate formed initially disappeared. The solution was then basified with KOH (0.8 M). The nanoparticles were suspended in this solution with the aid of an ultrasonic bath for 20 min. The initial ratio was 10 w% Ag and 90 w% CGO as this guarantees percolation in the final sintered sample. Finally, to initiate the reaction of reduction, 3 mL of dextrose solution (0.25 M) were added drop-wise to the mixture and left under stirring at room temperature for five minutes. The suspension was centrifuged and rinsed at least five times to eliminate all remaining reagents. The dry, clean, coated powders were pelletized (2.5 cm diameter) uni-axially and then cold-isostatically pressed (250 MPa) before being sintered at 1100 °C for 4 h. The pellets were polished at both surfaces with metallographic paper down to the final 1 mm thickness. The density and open porosity was measured with Archimedes' method using de-ionised water as the immersion fluid. The samples were boiled for 1 h to ensure all open porosity was filled with water.

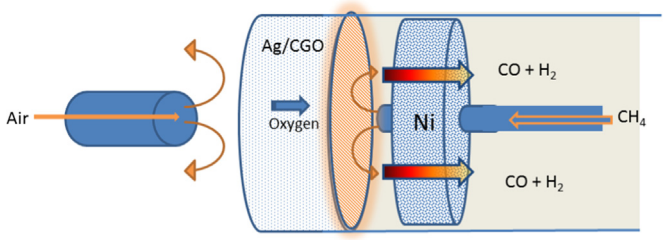

Fig. 2. Schematic of membrane partial oxidation reactor. The membrane was sealed to an alumina tube with an alumina based sealant. Air was blown on one side and methane diluted in argon was blown on the other side. A nickel mesh was placed close to the surface of the membrane to catalyse the reforming of methane.

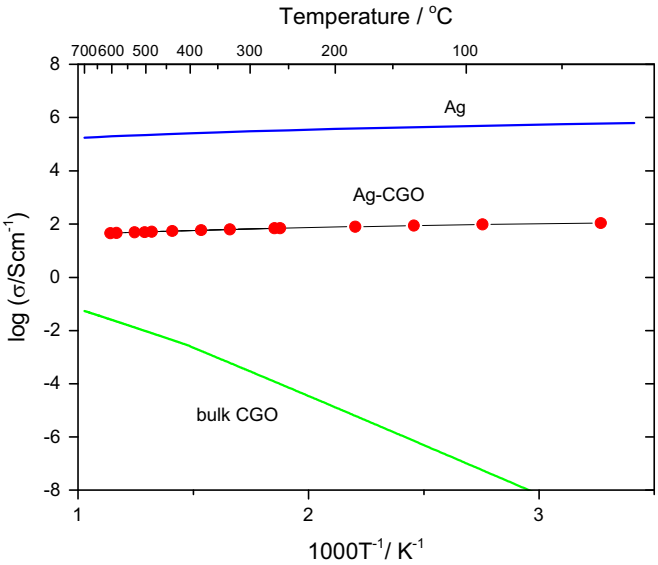

Fig. 3. Conductivity of the Ag/CGO composite and the literature values for silver (ASM International Handbook Committee, 1990) and CGO (Steele, 2000).

A Field Emission Gun Scanning Electron Microscope (FEG-SEM Gemini 1525) was used for imaging of the nano-composite materials. Images of fracture surfaces of the membranes were collected to check the dense nature of the samples and identify the presence of any cracks or large pores. The distribution of silver, doped-ceria and pores were analysed, and this has been discussed in our previous report (Ruiz-Trejo et al., 2014). The crystallinity of the powders and consolidated samples was analysed with an X'Pert PRO MRD X-ray diffractometer and the composition was estimated using the Chung method (Chung, 1974).

A 1 mm thick pellet with surface area of 3.1 cm^2 was placed in an alumina tube and sealed around its periphery with an alumina-based ceramic sealant (Aron Ceramics, Japan). The sealed sample was kept at 500 °C overnight and then held and measured at each test temperature for one hour. One side of the pellet was fed with air at 130 mL min^{-1} at NTP (Normal Temperature and Pressure) conditions while the other side was swept with zero-grade argon or diluted methane at a rate of 100 mL min^{-1} at NTP conditions. The gases were of commercial purity (BOC, UK). The mass spectrometer was calibrated with separate certified mixtures of N_2 (1%), O_2 (2%) and CO_2 (1%) each diluted in argon; CH_4 was calibrated using mixtures made with mass flow controllers (Bronkhorst). The mass spectrometer was calibrated at the beginning of the each permeation experiment. Two permeation experiments were carried out both on the same disc.

For oxygen permeation measurements argon was used as sweep gas and this stream was analysed in a mass spectrometer (Prolab Benchtop) connected downstream. The oxygen leaks into the sweep gas were taken into account by measuring the amount of nitrogen in the permeate side and assuming it leaks in gaseous form with the same composition as air. The oxygen flux reported is the oxygen flux measured minus the oxygen leaks; the corrected value is then the oxygen permeating through the membrane solely by solid state transport. The temperature range investigated was 550–800 °C.

A diagram of the set-up used for partial oxidation is shown in Fig. 2. A piece of nickel foam (Goodfellow, 1.6 mm thick, external area 2.8 cm^2, porosity 95%, and purity 95%) was placed directly in contact with the membrane on the oxygen-lean side as a catalyst. Four compositions of methane were used: 1.8%, 2.5%, 3% and 4% diluted in argon and with a total flow rate of 100 mL min^{-1} at NTP. The gas analysis was performed on the methane stream. To check for carbon deposition, Raman spectroscopy was used after the experiments (Horiba Jobin Yvon LabRAM 800 h Raman Spectrometer). The temperature range tested was 500–700 °C unless otherwise indicated; the composite tested was run at least 48 h at $T > 500$ °C in a pure methane environment. Leaks from air to the permeate side were assumed to be similar to the pure oxygen permeation experiments where N_2 can be measured unambiguously; leaks of methane to the air side are considered to be minimal as demonstrated in the case of H_2 leaking to the air side in Ag/CSO membranes (Ruiz-Trejo et al., 2014).

3. Results

The XRD data showed no signs of reaction between CGO and silver before or after sintering. The large surface area of the ultrafine

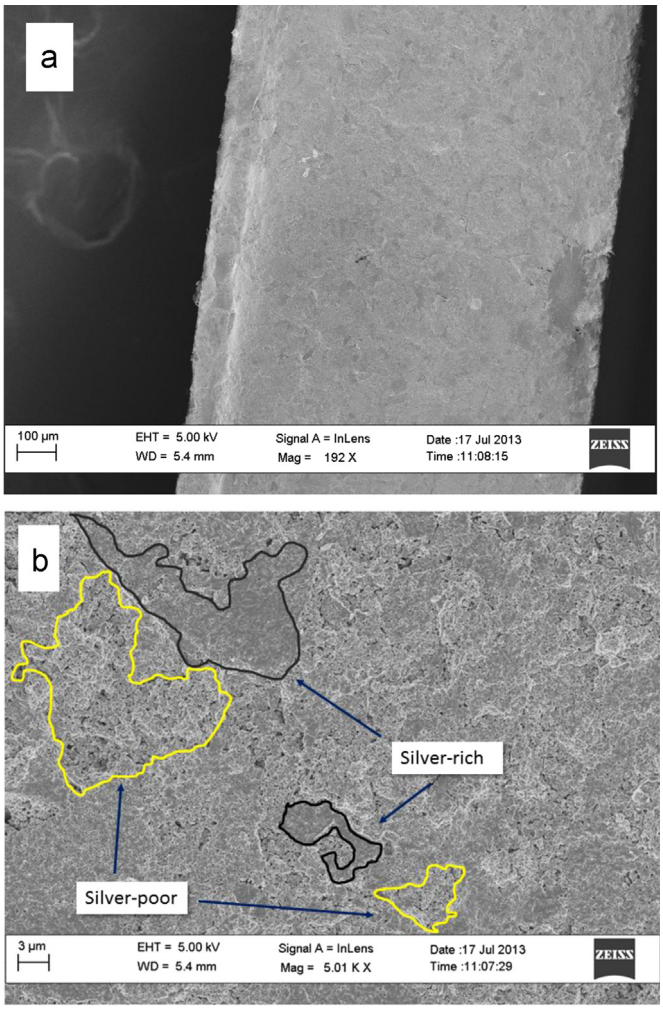

Fig. 4. (a) Fracture cross-section of a Ag/CGO membrane having a silver content of 7 vol% and (b) higher magnification of a cross-section of the membrane highlighting silver rich and silver poor regions.

Table 1
Mol percentage of reactants and products of the partial oxidation of methane. The percentage of conversion and selectivity is also shown. The total flow was 100 mL min^{-1} (NTP) and the balance was argon.

$T/^{\circ}C$	$[CH_4]_{fed}$	$[CO_2]_{detected}$	$[CH_4]_{consumed}$	$[CO]_{produced}$	% Conversion	% CO selectivity
500	1.8	0.028	0.117	0.089	6.5	76
	2.5	0.023	0.247	0.225	9.8	91
	3	0.016	0.397	0.382	13.2	96
	4	0.012	0.609	0.597	15.2	98
600	1.8	0.040	0.462	0.422	25.6	91
	2.5	0.046	0.642	0.596	25.6	93
	3	0.050	0.755	0.706	25.1	93
	4	0.058	0.938	0.880	23.4	94
700	1.8	0.072	0.474	0.403	26.3	85
	2.5	0.067	0.606	0.540	24.2	89
	3	0.062	0.685	0.623	22.8	91
	4	0.068	0.835	0.768	20.8	92

particles of CGO are used as the driving force to sinter the material at the relatively low temperatures needed to avoid excessive loss of silver. The distribution of the different phases has been analysed in our previous work using FIB-SEM tomography (Ruiz-Trejo et al., 2014). The silver content of the membrane was 7 vol% from XRD analysis and its density was 7.02 g cm^{-3} by Archimedes' method, which corresponds to 95% of the expected theoretical density of 7.37 g cm^{-3} for this Ag/CGO composition. The open porosity obtained by water displacement was 2% and was measured in the sample used for the permeation experiments. It should be noted that the detection of open porosity does not imply that the pores percolate the thickness of the membrane.

Fig. 3 shows the measured conductivity of the composite Ag/CGO in air and the values for silver metal conductivity and CGO bulk ionic conductivity in air (ASM International Handbook Committee, 1990; Steele, 2000). The bulk membranes were metallic despite the low level of silver content; however the lowest silver content required to achieve percolation has not yet been determined. Nonetheless, our fabrication technique led to percolation of the silver well below the value of 30 vol% usually taken as the minimum. At room temperature the conductivity was *ca* 100 s cm^{-1} and at 600 °C the electronic conductivity was *ca* 44 s cm^{-1}, at least three orders of magnitude larger than the bulk ionic conductivity of the CGO, indicating that the latter is the rate limiting process for oxygen transport in the composite.

Fig. 4a shows the SEM microstructure of a typical membrane. Fig. 4b shows the two regions that are produced during sintering: a very dense silver-rich CGO and one that is silver-poor with more porosity visible. A more detailed analysis of this characteristic was carried out in our previous work (Ruiz-Trejo et al., 2014). Although there may be variations between Ag/CSO and Ag/CGO two main points obtained in that work were: in the silver-rich regions (11.8 vol%) most of the silver was percolating with a low level of porosity (0.3 vol%) and in the silver-poor regions (4.5 vol%) the silver was not percolating and showed a high level of non-percolating porosity (4 vol%). An ideal membrane should be more homogenous and be similar to the silver-rich regions: dense and percolating. The presence of two regions is probably an indication that the nanoparticles were not coated individually but rather agglomerates of CSO were coated leading to an uneven distribution of silver. To achieve a single region it might be necessary to percipitate silver directly into the suspension of the nanoparticles as obtained after cleaning the suspension obtained via CHFS. An optimisation of this process is underway.

For the partial oxidation experiments, the detection of the reactants and products was carried out with a mass spectrometer and it was assumed that the carbon-containing products from methane were only CO and CO_2 since no carbon deposition was detected by Raman spectroscopy. It was further assumed that there were no other processes such as oxidative coupling of methane although this deserves future investigation (Tenelshof et al., 1995). The species unambiguously detected and calibrated were CH_4 and CO_2 and these were used to estimate the amount of CO produced according to Eqs. (5)–(8). The oxygen permeated in the methane oxidation experiments was estimated with Eq. (9), where unwanted oxygen leaks come from air at the same rate as measured in the oxygen permeation experiment. The concentration of H_2O was not measured and therefore only a lower boundary level for the oxygen permeation rate can be estimated, *i.e.* $[H_2O]$ in Eq. (9) is assumed to be zero.

$$[CH_4]_{consumed} = [CH_4]_{fed} - [CH_4]_{detected} \quad (5)$$

$$[CO]_{produced} = [CH_4]_{consumed} - [CO_2]_{detected} \quad (6)$$

$$CH_4 conversion\% = \frac{[CH_4]_{consumed}}{[CH_4]_{fed}} 100 \quad (7)$$

$$COselectivity\% = \frac{[CO]_{produced}}{[CH_4]_{consumed}} 100 \quad (8)$$

$$[O_2]_{permeated} = [CO_2]_{detected} + \tfrac{1}{2}[CO]_{Produced} + \tfrac{1}{2}[H_2O] - \tfrac{20.9}{79.1}[N_2] \quad (9)$$

Table 1 shows the results of the partial oxidation products with the flow of methane feed also tabulated.

After operation for 48 h, the experiments were stopped and the absence of carbon deposition on the composite was first tested by visual inspection and then evaluated with Raman spectroscopy on the surface of the membrane, however no coking was observed by either method. However, longer term stability tests are needed to determine a useful temperature range of operation since at higher temperature silver exudation might be a problem as will be shown later.

Fig. 5 shows the percentage CO selectivity for various temperatures and input flows of methane. Although there is some non-linearity, the high selectivity observed for the production of carbon monoxide under all conditions is significant, proving that partial oxidation of methane was achieved, the main goal of this study. The selectivity seems to generally decrease with increasing temperature and when the input methane flow is low, the reaction is less selective. These high selectivities were obtained despite the use of an un-optimised nickel mesh as a catalyst, and may be improved by employing a different catalyst.

Fig. 6 shows that the conversion increases from 500 to 600 °C as expected, however, the fact that the conversion does not increase between 600 and 700 °C suggests that other factors (such as: local temperature variations, microstructural changes, surface limitation, dynamic carbon-deposition/elimination, gas-phase reaction) may be affecting the reaction, and this requires further study.

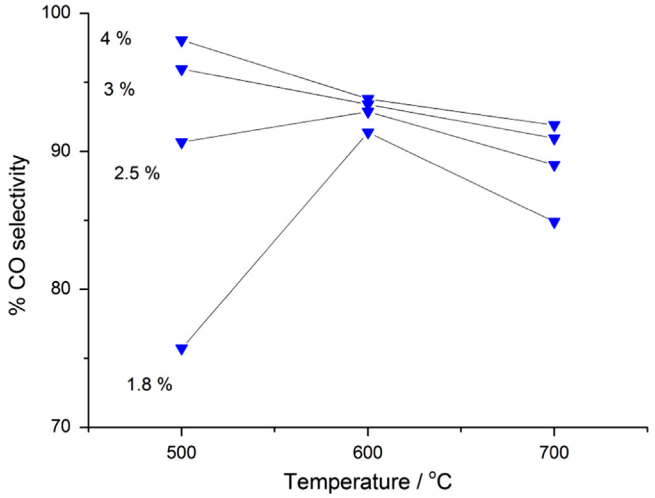

Fig. 5. Percentage of CO selectivity at different temperatures and CH_4 concentrations used (in mol%). The total flow fed was 100 mL min^{-1} (NTP) and the balance was argon.

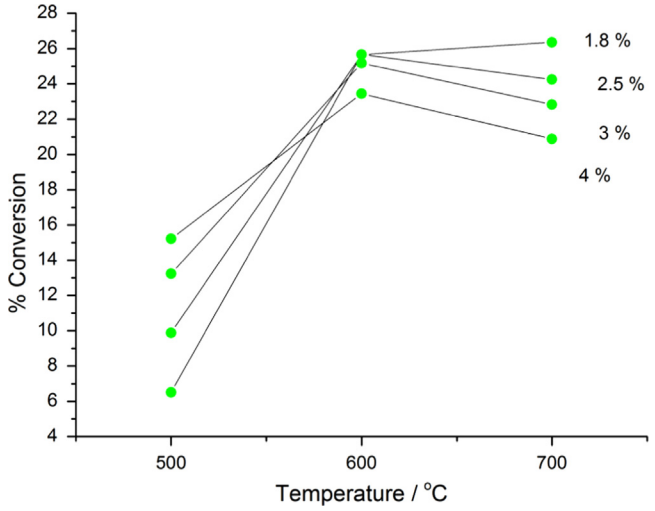

Fig. 6. Methane conversion as a function of temperature showing a general trend towards higher conversion at higher temperatures. CH_4 concentrations used are indicated as mol%.

The separation membrane was observed to degrade if operated in methane above 700 °C leading to lower conversion rates. One membrane was operated at 800 °C under methane after which droplets of silver were observed on the methane side as seen in Fig. 7a and to a lesser degree on the air side as shown in Fig. 7b. Although nominally both sides of the membrane were at the same temperature, heat released during the complete oxidation of methane has probably exacerbated the exudation of silver droplets.

Fig. 8 shows the oxygen flux measured by mass spectrometry using argon as the sweep gas (no methane), and also the lower bound oxygen flux with CH_4 present as calculated from the amounts of CH_4 consumed and CO_2 produced. The real oxygen flux in the latter case was expected to be higher as the oxygen transformed to water was not measured. A recent report for oxygen separation in Ag–CuO–CGO (1 mm thick) composites indicated oxygen fluxes of 0.05 mL cm^{-2} min^{-1} at 700 °C between N_2 and air. At the same temperature, our values reported here for argon as sweep gas are 0.015 mL cm^{-2} min^{-1}, but higher when the sweep gas was methane: 0.18 mL cm^{-2} min^{-1}.

The permeation from air was carried out before the partial oxidation experiment to determine the rate of oxygen flux and estimate unwanted leaks; oxygen flux increased with temperature as expected, but the values obtained remained close to the leakage value. However, with methane the oxygen flux increased by nearly an order of magnitude. Fig. 8 also indicates that a higher methane concentration led to higher permeation of oxygen.

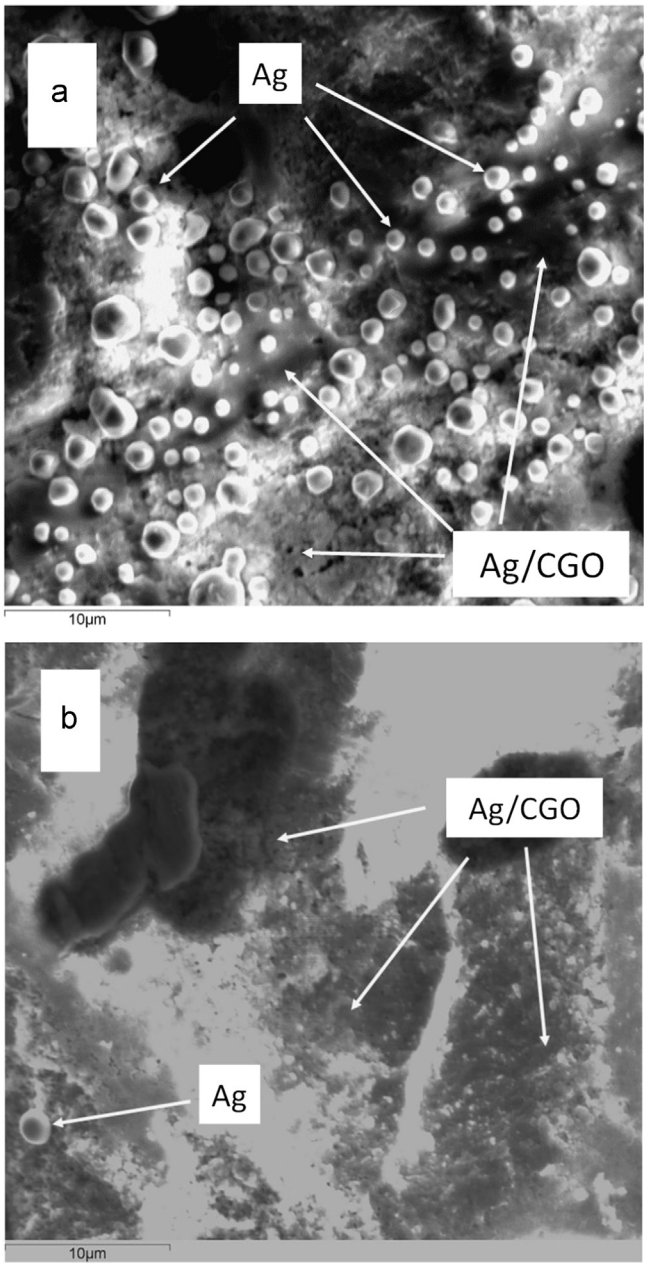

Fig. 7. (a) Ag/CGO surface of the methane side after operation at 800 °C for 1 h showing droplets of silver on top of the Ag/CGO membrane. (b) Ag/CGO surface exposed to air after operation at 800 °C for 1 h showing only one droplet of silver. Both sides had the same nominal temperature.

4. Discussion

The diffusion-controlled oxygen flux across the membrane depends, according to Wagner's theory, is given by

$$J_{O_2} = \frac{RT}{4^2F^2L}\sigma_i \ln\frac{p'_{O_2}}{p''_{O_2}} \quad (10)$$

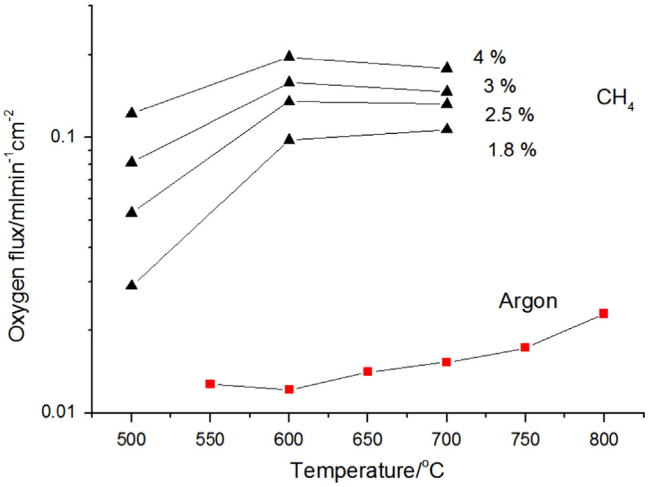

Fig. 8. Oxygen flux through the membrane with, and without, methane and nickel on the permeate side.

where σ_i is the ionic conductivity, L the thickness of the membrane, R is the gas constant, T the temperature and F Faraday's constant. Although this is a simplification, in that it does not consider the rates of reaction at the two membrane surfaces, this is a starting point to better understand some of the variables that control the flux of oxygen and consequently the partial oxidation of methane. Eq. (10) states that oxygen permeation can be increased by either decreasing the thickness of the membrane or by decreasing the chemical potential of oxygen in the sweep side of the membrane. The latter is achieved by introducing methane as seen in the large increase in oxygen flux observed when the methane concentration was increased (see Fig. 8). Sweeping with hydrogen has also been shown to increase the oxygen flux in similar composites (Ruiz-Trejo et al., 2014). The authors are currently investigating alternative fabrication routes for yet thinner membranes.

Eq. (10) does not consider a surface controlled permeation. In previous work we have estimated that for thicknesses above 300–500 μm the flux should be controlled by bulk diffusion (Ruiz-Trejo et al., 2014), therefore, the membrane studied herein probably operates in a bulk-diffusion controlled regime when argon is fed. However, when methane is fed the oxygen flux limitation may be different since the surface rate constant at the oxygen lean side is not known. We can estimate the theoretical value of oxygen flux calculating first the pO_2 in the permeate side using the equilibrium

$$CO + \tfrac{1}{2}O_2 \rightarrow CO_2 \qquad (11)$$

with an equilibrium constant of *ca* $\ln K = 26.4$ at 700 °C (Ellingham, 1944). For a feed with 4% methane, $[CO_2]$ is 0.068% and [CO] is 0.768% (from Table 1), the pO_2 value is 9.2×10^{-26} atm, the ionic conductivity is 0.045 s cm^{-1} (Steele, 2000) and the expected flux is then 1.9 mL min^{-1} cm^2, an order of magnitude higher than the measured value 0.18 mL min^{-1} cm^2. In addition to the uncertainty associated with the amount of oxygen converted to H_2O, the difference might be indicating that the oxygen flux was being limited by surface reaction on the permeate side. At lower temperatures the difference was less dramatic: at 500 °C, 0.43 mL min^{-1} cm^2 as expected, while 0.12 mL min^{-1} cm^2 was measured as the lower boundary value. As future work will require thinner membranes to increase oxygen permeation rates, spectroscopic *in-situ* and mechanistic studies are needed to understand the surface evolution/oxidation reactions in CH_4 environments.

Although we did not observe any carbon deposition post test, this may still have happened during operation. Work under CH_4 or CO/CO_2 mixtures in fuel cells and electrolysers is often plagued with problems of carbon deposition, however, the capability of ceria-based compounds to oxidise carbon is well-known (Aneggi et al., 2012; Trovarelli, 2002). Furthermore, silver is a well-known catalyst for partial oxidation reactions (Nagy and Mestl, 1999). It is then expected that both silver and ceria profit from each other's capabilities, making them an encouraging combination in membrane reactors for partial oxidation reactions.

5. Conclusions

Methane has been partially oxidised using novel Ag/CGO composites membranes. These were manufactured by sintering CGO nanoparticles prepared by CHFS and then coated with silver. The oxygen permeation through the membrane from air to argon as sweep gas, was estimated to be 0.02 mL cm^{-2} min^{-1} (NTP) at 700 °C, while using a CH_4-containing atmosphere on the low oxygen activity side, the permeation rate was greater than 0.18 mL cm^{-2} min^{-1} (NTP). At 700 °C, high selectivity for CO ($>90\%$) was observed and good methane conversion was measured (approximately 21%), and despite the simplicity of the reactor and the thickness of the membrane. The samples operated at CH_4 for at least 48 h below 700 °C without being mechanically compromised, however if operated at 800 °C, silver exuded to the surface as a consequence of the heat released during methane oxidation. Due to the stability of CGO in carbon atmospheres, the Ag/CGO composites are expected to function well in these reducing atmospheres and under large transmembrane pO_2, differences but operation at higher temperatures or in the presence of very exothermic reactions might lead to exudation of the silver.

Acknowledgements

ERT would like to thank EPSRC under the project Advancing Biogas Utilization through Fuel Flexible SOFC. JLMH acknowledges support through a UROP-grant from ESE-IC. We thank V. Duboviks for the Raman measurements.

References

ASM International Handbook Committee, 1990. ASM Handbook—Properties and Selection: Nonferrous Alloys and Special-Purpose Materials. vol. 2. ASM International, Materials Park, Ohio.
Aneggi, E., de Leitenburg, C., Llorca, J., Trovarelli, A., 2012. Catal. Today 197, 119.
Arnold, M., Wang, H.H., Feldhoff, A., 2007. J. Memb. Sci. 293, 44.
Balachandran, U., Dusek, J.T., Mieville, R.L., Poeppel, R.B., Kleefisch, M.S., Pei, S., Kobylinski, T.P., Udovich, C.A., Bose, A.C., 1995. Appl. Catal. A-Gen. 133, 19.
Bouwmeester, H.J.M., Burggraaf, A.J., 1996. In: Gellings, P.J., Bouwmeester, H.J.M. (Eds.), The CRC Handbook of Solid State Electrochemistry. CRC Press, Boca Raton, Florida, p. 481.
Bucher, E., Egger, A., Caraman, G.B., Sitte, W., 2008. J. Electrochem. Soc. 155, B1218.
Chung, F.H., 1974. J. Appl. Crystallogr. 7, 519.
Dong, H., Shao, Z.P., Xiong, G.X., Tong, J.H., Sheng, S.S., Yang, W.S., 2001. Catal. Today 67, 3.
Dyer, P.N., Richards, R.E., Russek, S.L., Taylor, D.M., 2000. Solid State Ion. 134, 21.
Ellingham, H.J.T., 1944. J. Society of Chem. Ind. 63, 125.
Nagy, A., Mestl, G., 1999. Appl. Catal. A-Gen. 188, 337.
Ozawa, M., Kimura, M., Isogai, A., 1993. J. Alloys Compd. 193, 73.
Ramirez-Cabrera, E., Atkinson, A., Chadwick, D., 2002. Appl. Catal. B-Environ. 36, 193.
Ramírez-Cabrera, E., Atkinson, A., Chadwick, D., 2004. Appl. Catal. B: Environ. 47, 127.
Rostrup-Nielsen, J.R., Sehested, J., Nørskov, J.K., 2002. Advances in Catalysis. Elsevier p. 65.
Ruiz-Trejo, E., Boldrin, P., Lubin, A., Tariq, F., Fearn, S., Chater, R., Cook, S.N., Atkinson, A., Gruar, R.I., Tighe, C.J., Darr, J., Brandon, N.P., 2014. Chem. Mater. 26, 3887.
Samson, A.J., Søgaard, M., Hendriksen, P. Vang, 2014. J. Membr. Sci. 470, 178.
Seeharaj, P., Atkinson, A., 2011. Solid State Ion. 204, 46.
Shao, Z.P., Yang, W.S., Cong, Y., Dong, H., Tong, J.H., Xiong, G.X., 2000. J. Membr. Sci. 172, 177.
Shao, Z.P., Xiong, G.X., Dong, H., Yang, W.H., Lin, L.W., 2001. Sep. Purifi. Technol. 25, 97.

Sousa-Aguiar, E.F., Noronhac, F.B., Faro, A., 2011. Catal. Sci. Technol. 1, 698.
Steele, B.C.H., 2000. Solid State Ion. 129, 95.
Sunarso, J., Baumann, S., Serra, J.M., Meulenberg, W.A., Liu, S., Lin, Y.S., da Costa, J.C. D., 2008. J. Membr. Sci. 320, 13.
Tenelshof, J.E., Bouwmeester, H.J.M., Verweij, H., 1995. Appl. Catal. A-Gen. 130, 195.
Teraoka, Y., Zhang, H.M., Furukawa, S., Yamazoe, N., 1985. Chem. Lett. 1743.
Tighe, C.J., Cabrera, R.Q., Gruar, R.I., Darr, J.A., 2013. Ind. Eng. Chem. Res. 52, 5522.
Tollens, B., 1882. Ber. Dtsch. Chem. Ges. 15, 1635.
Trovarelli, A., 2002. Catalysis by Ceria and Related Materials. Imperial College Press, London.
Vente, J.F., McIntosh, S., Haije, W.G., Bouwmeester, H.J.M., 2006. J. Solid State Electrochem. 10, 581.
Yu, A.S., Vohs, J.M., Gorte, R.J., 2014. Energy Environ. Sci. 7, 944.